Dual roles of Munc18-1 rely on distinct binding modes of the central cavity with Stx1A and SNARE complex

Lei Shi, Daniel Kümmel, Jeff Coleman, Thomas J. Melia, and Claudio G. Giraudo*
Department of Cell Biology, School of Medicine, Yale University, New Haven, CT 06520

ABSTRACT **Sec1/Munc18 proteins play a fundamental role in multiple steps of intracellular membrane trafficking. Dual functions have been attributed to Munc18-1: it can act as a chaperone when it interacts with monomeric syntaxin 1A, and it can activate soluble *N*-ethylmaleimide-sensitive factor attachment protein receptors (SNAREs) for membrane fusion when it binds to SNARE complexes. Although both modes of binding involve the central cavity of Munc18-1, their precise molecular mechanisms of action are not fully understood. In this paper, we describe a novel Munc18-1 mutant in the central cavity that showed a reduced interaction with syntaxin 1A and impaired chaperone function, but still bound to assembled SNARE complexes and promoted liposome fusion and secretion in neuroendocrine cells. Soluble syntaxin 1A H3 domain partially blocks Munc18-1 activation of liposome fusion by occupying the Munc18-1 central cavity. Our findings lead us to propose a transition model between the two distinct binding modes by which Munc18 can control and assist in SNARE-complex assembly during neurotransmitter release.**

Monitoring Editor
Thomas F.J. Martin
University of Wisconsin

Received: Feb 22, 2011
Revised: Aug 19, 2011
Accepted: Sep 1, 2011

INTRODUCTION

Membrane vesicles traffic proteins and lipids through different compartments of the cell (Bonifacino and Lippincott-Schwartz, 2003). Soluble *N*-ethylmaleimide-sensitive factor attachment protein receptors (SNAREs) are responsible for bringing both vesicle and target compartment membranes together and for catalyzing fusion by assembling into a four-helix complex (Sutton *et al.*, 1998; Weber *et al.*, 1998; Hu *et al.*, 2003). During synaptic transmission, syntaxin 1A/SNAP-25 (target organelle SNARE [t-SNARE]) on the plasma membrane and VAMP2 (vesicular SNARE [v-SNARE]) on synaptic vesicles are assisted or regulated by several proteins in vesicle docking and priming and in the final fusion steps (Rosenmund *et al.*, 2003; Sudhof, 2004). These regulators include Munc18, Munc13, synaptotagmins, and complexins (Brose *et al.*, 1992; Augustin *et al.*, 1999; Fisher *et al.*, 2001; Reim *et al.*, 2001; Gerber *et al.*, 2008). Unlike synaptotagmin and complexin, which play an important role in Ca^{2+}-triggered neurotransmitter release (Tucker *et al.*, 2004; Giraudo *et al.*, 2006, 2009), Sec1/Munc18 (SM) is a universal regulator of both constitutive and calcium-regulated membrane fusion (Sudhof and Rothman, 2009). However, the precise molecular mechanism of action of Munc18 during membrane fusion is still controversial (Sorensen, 2009).

The four-helix bundle is believed to be the general structure that all SM proteins recognize (Shen *et al.*, 2007; Sudhof and Rothman, 2009). Structural studies indicate that Munc18-1 binds the closed form of syntaxin 1A (Stx1A), thereby hindering formation of SNARE complexes (Dulubova *et al.*, 1999; Misura *et al.*, 2000). Thus Munc18-1 is a negative regulator of SNARE-complex assembly and an inhibitor of membrane fusion. By contrast, genetic studies showed an essential positive role of Munc18-1 in neurotransmitter release (Wu *et al.*, 1998; Verhage *et al.*, 2000; Weimer *et al.*, 2003).

This article was published online ahead of print in MBoC in Press (http://www.molbiolcell.org/cgi/doi/10.1091/mbc.E11-02-0150) on September 7, 2011.

*Present address: Department of Pathology and Laboratory Medicine, The Children's Hospital of Philadelphia, University of Pennsylvania, Philadelphia, PA 19104.

Address correspondence to: Claudio G. Giraudo (giraudoc@email.chop.edu).

Abbreviations used: C8, PC12 control cells; cdv2, cytoplasmic domain of VAMP2; coIP, coimmunoprecipitation; DKD16, double-knockdown PC12 cells; ELISA, enzyme-linked immunosorbent assay; GST, glutathione *S*-transferase; hGH, human growth hormone; Munc18-4M, Munc18-1 R39A/K46A/M47A/K63A mutant; NBD, 7-nitro-2-1,3-benzoxadiazol-4-yl; Ni-NTA, Ni-nitrilotriacetic acid; NMR, nuclear magnetic resonance; PBS, phosphate-buffered saline; PSS, physiological saline solution; SM, Sec1/Munc18; SNARE, soluble N-ethylmaleimide-sensitive factor attachment protein receptors; Stx1A, syntaxin 1A; Stx1A H3-4M, Stx1A H3 domain D231A/E234A/N236A/D242A mutant; SUMO, small ubiquitin-like modifier; TC, isothermal titration calorimetry; t-SNARE, target organelle SNARE; v-SNARE, vesicular SNARE; wt, wild type; YFP, yellow fluorescent protein.

In addition, recent evidence from cell-free systems shows that Munc18-1 can bind SNARE complexes and activate liposome fusion (Scott *et al.*, 2004; Dulubova *et al.*, 2007; Rickman *et al.*, 2007; Shen *et al.*, 2007, 2010; Rodkey *et al.*, 2008; Diao *et al.*, 2010; Rathore *et al.*, 2010).

These apparent discrepancies among different studies suggest opposite roles of Munc18-1 (Toonen and Verhage, 2007; Sorensen, 2009; Carr and Rizo, 2010) in membrane fusion. Binding of Munc18-1 to the closed form of Stx1A, has been associated with its chaperone function, which seems to be critical in helping the trafficking of Stx1A from the ER to the plasma membrane (Rowe *et al.*, 1999, 2001; Salaun *et al.*, 2004; Arunachalam *et al.*, 2008; Han *et al.*, 2009; Malintan *et al.*, 2009). After Stx1A arrives at the target site, it is thought that Munc18-1 promotes the SNARE-complex assembly, which facilitates membrane fusion (Shen *et al.*, 2007). To reconcile these different roles of Munc18-1, dual modes of binding of Munc18-1 to Stx1A and SNARE complexes have been proposed (Khvotchev *et al.*, 2007; Rickman *et al.*, 2007; Shen *et al.*, 2007). However, the differences between these two modes and how these modes link to each other are unknown.

In this work, on the basis of the crystal structure of Munc18-1/Stx1A complex, we identify key residues within the Munc18-1 central cavity (Misura *et al.*, 2000; Burkhardt *et al.*, 2008), that make contact with Stx1A-H3 domain and affect the normal trafficking to the plasma membrane in vivo. Mutations of these residues in Munc18-1 lead to a reduction in the interactions with Stx1A and impaired chaperone function. However, such mutations appear not to affect the binding to SNARE complexes and the ability to activate SNARE-mediated liposome fusion. In addition, we found that the Stx1A H3 domain binds to Munc18-wild-type (Munc18-wt), but not to Munc18 mutant, and competes with SNARE complex for binding to the central cavity of Munc18-1, thus conferring resistance to Munc18-1 activation in liposome fusion. We suggest a transition model in which Munc18-1 executes its dual roles by using two different binding modes of its central cavity to engage Stx1A and SNARE complexes.

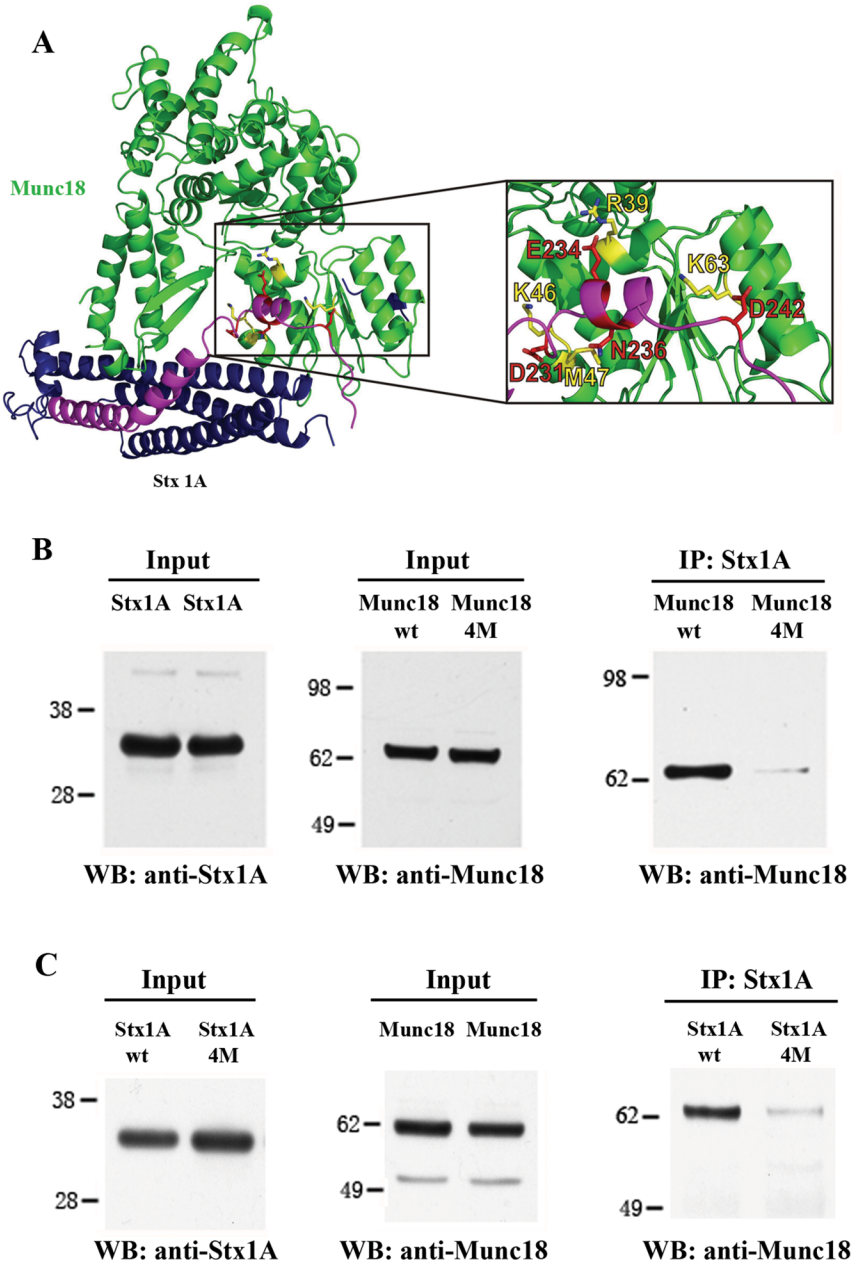

FIGURE 1: Munc18-4M mutant binds poorly to Stx1A. (A) Cocrystal structure of Munc18 (green)-Stx1A (Habc domain: blue; H3 domain: purple): the C-terminal half of the Stx1A H3 domain inserts deeply into the Munc18 central cavity; the residues R39/K46/M47/K63 (highlighted in yellow) within the Munc18 central cavity make close contacts with residues D231/E234/N236/D242 (red) within the Stx1A H3 domain. (B) coIP experiments using HeLa cells transiently transfected with Stx1A and either Munc18-wt or Munc18-4M mutant (R39A/K46A/M47A/K63A). (C) coIP experiments using HeLa cells transiently transfected with Stx1A-wt or Stx1A-4M mutant and Munc18-wt. Blots are representative of three independent experiments.

RESULTS

Munc18-1 quadruple mutant has poor interaction with Stx1A and cannot traffic Stx1A to the plasma membrane in PC12 cells

To determine which residues of Munc18-1 are mainly responsible for the interaction between Munc18-1 and the monomeric Stx1A, we analyzed the cocrystal structure of Munc18-Stx1A (Misura *et al.*, 2000). In this crystal structure, the Stx1A H3 domain (also known as the core domain or SNARE motif) is twisted, and its C-terminal half is inserted deeply into the central cavity of Munc18-1 (Figure 1A). This unique arrangement suggests there is a strong interaction between Munc18-1 and the Stx1A H3 domain. We calculated the distances between residues on Munc18-1 and on Stx1A H3 domain using the software CNS (Brunger *et al.*, 1998; http://cns-online.org/v1.3). We identified several candidate residues with distances smaller than 4 Å that could potentially be engaged in a physical interaction (Supplemental Table S1). Based on their proximity and on the amino acid side chain charges, the residues Arg-39, Lys-46,

Met-47, and Lys-63 on Munc18-1 (Figure 1A) were the best candidates to be further investigated. We tested the contributions of residues R39, K46, M47, and K63 on the interaction with Stx1A by coimmunoprecipitation (coIP) experiments in HeLa cells. Results showed that R39A and K46A/M47A mutations in Munc18 slightly reduced the binding to Stx1A, while K63A mutation partially reduced the amount of Stx1A coimmunoprecipitated (Supplemental Figure S1A). Previous studies using the two-hybrid system tested the single mutants R39C and K63E and did not show any significant effect on the interaction with Stx1A, while mutation K46E presented ~50% reduction in Stx1A binding (Han *et al.*, 2009).

To generate a mutant displaying a clear phenotype of Stx1A binding, we generated a Munc18-1 quadruple mutant in which these four residues were simultaneously mutated: R39A/K46A/M47A/K63A (Munc18-4M). We tested the interaction of this mutant with Stx1A by coIP experiments in HeLa cells. Results of these experiments showed the ability of Munc18-4M to interact with Stx1A was dramatically reduced compared with Munc18-wt (Figure 1B). Similar results were obtained in the reciprocal coIP using Munc18-wt and Stx1A-4M mutant. In this Stx1 mutant, the complementary residues of Stx1A-H3 domain that interact with the residues mutated in Munc18-4M have been mutated to alanine (D231A/E234A/N236A/D242A; Figure 1C). Isothermal titration calorimetry (ITC) experiments showed that the affinity of Munc18-4M for Stx1A (K_d = 362.0 nM) is ~250 times lower than the affinity of Munc18-wt for Stx1A (K_d = 1.3 nM; Figure S1, B and C). Therefore residues R39/K46/M47/K63 in Munc18 appear to constitute some of the critical contact points with which Stx1A interacts.

To investigate whether residues R39/K46/M47/K63 play a critical role in Munc18-1 chaperone function, we tested the trafficking of Stx1A to the plasma membrane in rescue experiments using Munc18-1/-2 double-knockdown PC12 cells (DKD16), as described by Han *et al.* (2009). In PC12 control cells (C8), Stx1A displayed an evident plasma membrane localization (Han *et al.*, 2009; Figure 2, A–C). In contrast, in DKD16 cells, the transport of Stx1A to the plasma membrane was severely disrupted and most of the Stx1A was retained in earlier compartments of the exocytic pathway (Han *et al.*, 2009; Figure 2E–G). Reintroduction of Munc18-wt into the DKD16 knockdown cells dramatically reduced the Stx1A aggregates inside the cell and rescued normal localization of Stx1A back onto the plasma membrane (Figure 2, I–K), whereas transfection of DKD16 cells with Munc18-4M had no significant effect in rescuing the plasma membrane localization of Stx1A (Figure 2, M–O). The different rescuing ability of Munc18-wt and Munc18-4M was quantified by analyzing the fluorescence intensity along a cross-section of individual transfected cells (Figure 2, D, H, L, and P). The statistical analysis of the fluorescence intensity plots showed that Munc18-wt efficiently restored Stx1A plasma membrane localization; however, Munc18-4M was not able to significantly rescue plasma membrane localization of Stx1A when compared with mock-transfected cells (DKD16; Figure 2Q). To rule out the possibility that this difference is due to different expression levels of Munc18-wt and Munc18-4M in the transfected cells, we tested their expression levels in PC12 cells by Western blotting. Results showed that the level of expression of Munc18-4M was ~35% lower than Munc18-wt (Figure S2). However, it is unlikely that this difference could be responsible for the fivefold reduction of Stx1A to the plasma membrane. To further examine the functional properties of Mun18-4M, we also tested its ability to restore secretion in DKD16 cells using a previously described human growth hormone (hGH) secretion assay (Chung *et al.*, 1999). In these experiments, DKD16 cells were transiently transfected with the hGH reporter construct and either Munc18-wt, Munc18-4M, or Munc18-4M and Stx1A. Cells were incubated in the presence or absence of a high K^+ buffer to stimulate granule secretion, and the amount of hGH secreted to the media was determined by enzyme-linked immunosorbent assay (ELISA). Munc18-wt, but not Munc-8-4M, was able to significantly restore hGH secretion upon high K^+ stimulation (Figure 2R). Interestingly, when Munc18-4M was overexpressed with Stx1A, a partial recovery in hGH secretion was observed. Altogether, these results suggest that residues R39/K46/M47/K63 not only are critical for the physical interaction with Stx1A but also are essential for the chaperone function of Munc18-1 that facilitates the trafficking of Stx1A to the plasma membrane to undergo normal hGH secretion in PC12 cells.

Munc18-4M mutant can bind SNARE complexes and promote liposome fusion

Previous biochemical and nuclear magnetic resonance (NMR) studies have shown that Munc18-1 can not only bind Stx1A but also t-SNARE and SNARE complexes (Dulubova *et al.*, 2007; Deak *et al.*, 2009; Xu *et al.*, 2010). The latter binding mode activates SNARE-mediated membrane fusion in reconstituted systems, such as in the liposome fusion assay (Shen *et al.*, 2007; Rodkey *et al.*, 2008). To explore in detail the functional implications of mutating residues R39/K46/M47/K63 in Munc18-1, we compared the ability of Munc-8-4M and Munc18-wt to bind t-SNARE and SNARE complexes using a pulldown assay. For these experiments, we used coexpressed Stx1A and SNAP25 as a t-SNARE to pull down Munc18-wt or Munc-8-4M mutant. No significant difference was observed between the amount of Munc18-wt and Munc18-4M bound to immobilized t-SNARE (Figure 3A). A similar experiment was performed using a SNARE complex preformed with the same t-SNARE as above, and the cytoplasmic domain of VAMP2 (cdv2). Munc18-4M was able to bind SNARE complex to almost the same extent as Munc18-wt did (Figure 3A). Additionally, in liposome coflotation experiments, Munc18-wt and Munc18-4M cofloated with similar efficiencies when preassembled SNARE complexes were embedded in the liposomes (Figure S3, A and B). These results strongly indicate that the ability of Munc18-4M to bind t-SNARE and SNARE complexes has not been compromised.

To analyze whether other functional properties of Munc18-4M were affected, we tested the capacity of Munc18-4M to activate SNARE-mediated membrane fusion using the liposome fusion assay. Both Munc18-wt and Munc18-4M were able to stimulate the fusion reaction in a dose-dependent manner, showing little significant difference (Figures 3B and S3C).

It has been shown that Munc18-1 promotes liposome fusion by acting on partially assembled SNARE complex (Shen *et al.*, 2007). Once Munc18-1 binds these preassembled SNARE complexes, the cdv2 cannot prevent these preassembled liposomes from fusing anymore, even though cdv2 almost completely blocks the fusion mediated by unpaired SNAREs (Shen *et al.*, 2007). To rule out the possibility that Munc18-4M could differentially affect the activation on the newly formed SNARE complexes but not on partially assembled complexes, we added cdv2 just before starting the fusion reaction. These experiments showed that addition of cdv2 to the fusion reaction in the absence of Munc18-1 drastically reduced the extent of fusion to the background levels. In contrast, preassembled fusion levels were similar when the liposomes were preincubated with either Munc18-wt or Munc18-4M in the presence of cdv2 (Figure 3C).

Based on our results for the coIP, ITC, and in vivo experiments, Munc18-1 appears to have two distinct binding modes: the Munc18-Stx1A binding mode, in which the contacting residues R39/K46/M47/K63 located within the central cavity of Munc18-1 are critical

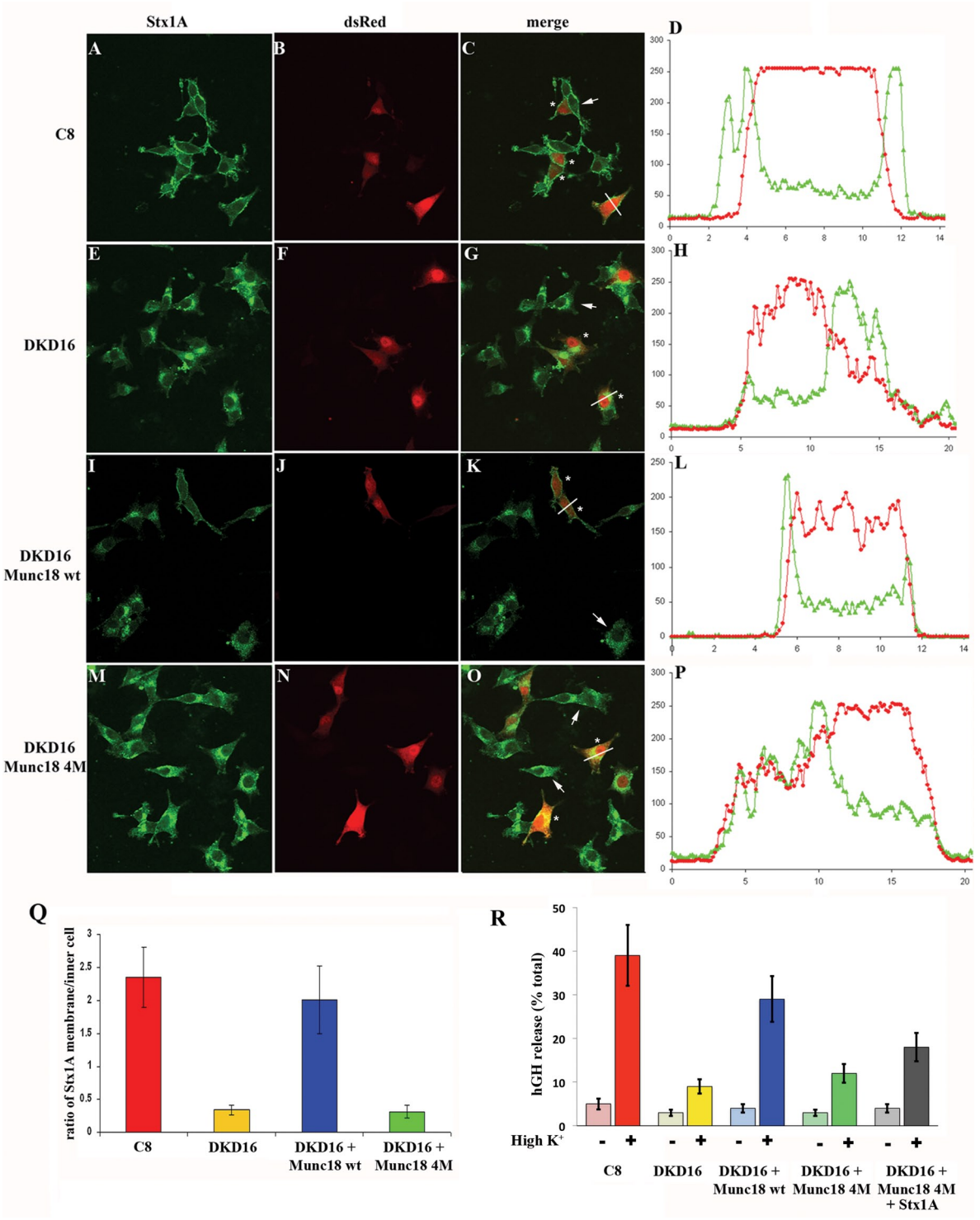

FIGURE 2: Munc18-4M mutant cannot efficiently traffic Stx1A to the plasma membrane in PC12 Munc18-1/-2 double-knockdown cells (Han *et al.*, 2009). (A–C) Stx1A localized on the plasma membrane in C8 control cells, whereas Stx1A mostly localized within the secretory pathway in DKD16 knockdown cells (E–G). Reintroduction of Munc18-wt rescued the phenotype and relocalized Stx1A back onto plasma membrane (I–K). Expression of Munc18-4M mutant had no rescue function, and Stx1A was still retained inside the cell (M–O). Asterisks, transfected cells; arrows, nontransfected cells. The DsRed-N1vector was used as cotransfection marker. Fluorescence intensity distribution (D, H, L, and P) along the white line in the transfected cell (C, G, K, and O). Quantification of the fluorescence intensity distribution plots calculated as the ratio between: the mean fluorescence intensity at the borders of the cell over the fluorescence intensity at the middle distance of the borders (Q). Results are mean ± SD of two independent experiments (n = 50). (R) hGH secretion assay using C8 or DKD16 cell lines cotransfected with a plasmid coding for hGH-YFP construct and either Munc18-wt, Munc18-4M, Munc18-4M and Stx1, or without Munc18. Cells were stimulated with or without high K^+ buffer for 15 min at 37°C. After cells were pelleted, the release of hGH to the medium was quantified by ELISA as percentage of the total content of hGH in each well. Results are mean ± SD of two independent experiments; each condition was run in triplicate.

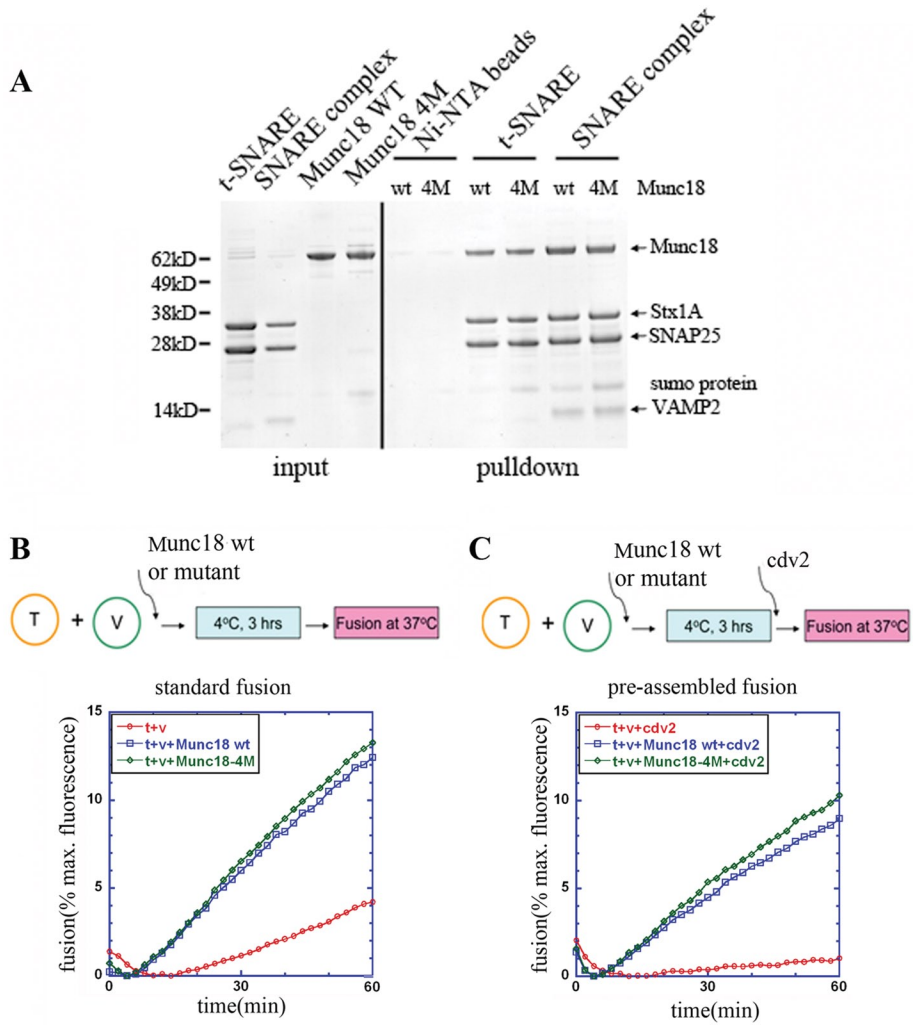

FIGURE 3: Munc18-4M mutant can bind the SNARE complexes and promote liposome fusion. (A) Pulldown experiment to test binding of Munc18-wt or Munc18-4M mutant to immobilized His-tagged t-SNARE or SNARE complex. Munc18-wt and Munc18-4M proteins were expressed as His6x-SUMO-construct and purified using Ni-NTA beads following SUMO-protease cleavage. Briefly, for pulldown experiments, His-tagged t-SNARE or SNARE complex was immobilized on the Ni-NTA beads and incubated with either Munc18-wt or Munc18-4M. Bound fractions were analyzed by SDS–PAGE followed by Coomassie staining. Note that the SUMO protein recovered on the bound fractions corresponds to the His-SUMO-tag that copurified as contaminant of Munc18 proteins, as it is also observed in the input lanes of the gel. (B) Standard liposome fusion in the absence or presence of 5 μM Munc18-wt or Munc18-4M mutant. (D) Preassembled liposome fusion assay in which the v- and t-liposomes were preincubated for 3 h at 4°C in absence or presence of 5 μM Munc18-wt or Munc18-4M mutant; subsequently, cdv2 was added before starting the fusion reaction to prevent the assembly of newly formed SNARE complexes.

for the physical interaction with Stx1A and for the in vivo chaperone function; and the Munc18–SNARE complex interaction, which is required for the activation of the liposome fusion reaction. Although it is believed that the central cavity is also involved in the interaction with the SNARE four-helix bundle, the residues R39/K46/M47/K63 do not appear to be crucial for SNARE-complex binding or for the activation of the liposome fusion reaction.

Stx1A H3 domain and SNARE complex compete for Munc18-1 binding

Our studies indicate that the binding of the Stx1A H3 domain to the central cavity of Munc18-1 significantly contributes to the Munc18-Stx1A interaction. The Munc18 central cavity is believed to be the binding site for SNARE complexes as well (Shen *et al.*, 2007; Xu *et al.*, 2010). To determine whether the Stx1A H3 domain binds to Munc18 and competes with the SNARE four-helix bundle for binding to the Munc18 central cavity, we performed pulldown experiments in which glutathione *S*-transferase (GST)-Stx1-H3 soluble domain (residues 191–253) was immobilized to Sepharose beads and incubated with either Munc18-wt or Munc18-4M. Munc18-wt, but not Munc-8-4M, specifically bound to the GST-Stx1-H3 beads, as is shown by Western blotting (Figure 4A). Moreover, the bound fraction of Munc18-wt decreased in a dose-dependent manner when increasing concentrations of SNARE complexes were added to the reaction (Figure 4, A and B). These results strongly suggest that the mutations lining the central cavity in Munc18-4M are important for the interaction with Stx1 H3 domain and that Stx1 H3 domain competes with the SNARE complex for the same binding region.

Additionally, we examined the effect on Munc18-wt activation of liposome fusion when soluble Stx1A H3 domain is added. Our findings indicate that the Stx1A H3 domain itself did not change the liposome fusion after being coincubated with the t-/v-liposomes on ice for 3 h (Figure S4A). However, when the Stx1A H3 domain was coincubated with Munc18-1 and t-/v-liposome before the fusion reaction, we found that the Stx1A H3 domain inhibited ~50% of Munc18-wt activation (Figure 4C). In addition, we performed dose–response experiments, and the initial rate of the liposome fusion reaction was used to measure Munc18-1 activation (Shen *et al.*, 2007). We found that the Stx1A H3 domain reduced the initial fusion rate of Munc18-1 activation more than 40% (Figure 4D). In these experiments, maximum inhibition was probably limited by the oligomerization of the Stx1A H3 domain at concentrations higher than 5 μM. The Stx1A H3 domain also reduced the Munc18-1 activation of preassembled SNARE complexes in the liposome fusion assay by ~50% (Figure 4C), suggesting that fewer preassembled SNARE complexes were protected by Munc18-1 when the Stx1A H3 domain was present.

In addition to measuring Munc18-1 activation, we performed "order of addition" experiments in which t-/v-liposomes were incubated first with Munc18-1 alone, and then the Stx1A H3 domain was added just before the fusion reaction started (Figure 4E, H3 no coincubation). Under these conditions, Munc18-1 activation of liposome fusion was not affected by the Stx1A H3 domain, suggesting that Stx1A H3 domain can compete with partially assembled SNARE complexes, but not with fully assembled complexes, for binding Munc18 (Figure 4E). Similar results were obtained when we tested Munc18 activation on preassembled SNARE complexes. Therefore our data suggest that the Stx1A H3 domain inhibits

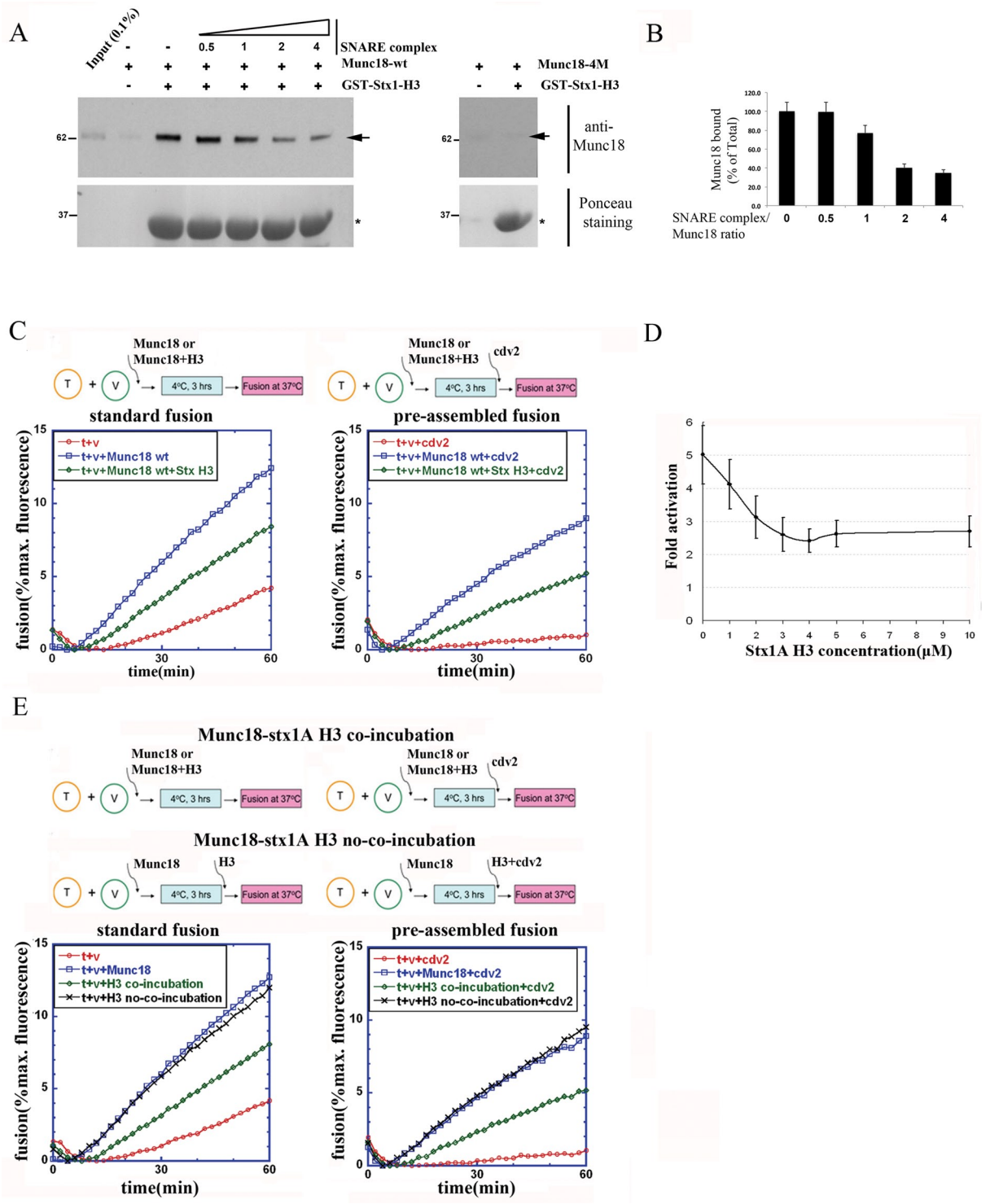

FIGURE 4: Stx1A H3 domain binds Munc18 and partially inhibits Munc18 activation of liposome fusion. (A) Equal amounts of either Munc18-wt or Munc18-4M were incubated with the glutathione beads in the presence or absence of GST-Stx1-H3 and in the presence or absence of increasing concentration of soluble SNARE complexes. Beads were washed, and the Munc18 bound fraction was determined by Western blotting using a polyclonal anti-Munc18 antibody. Arrows indicate the expected molecular weight of Munc18. Asterisks mark the expected molecular weight of GST-Stx1-H3 after Ponceau staining. The amount of soluble SNARE complexes added to the reaction (0.5, 1, 2, and 4) is indicated as SNARE complex/Munc18 ratio. (B) Quantification of Munc18 bound fraction in the competition experiment. Results are the mean ± SD of two independent experiments. (C) Standard and preassembled liposome fusion experiments performed in the absence or presence of 5 μM Munc18-wt alone or 5 μM Munc18 and 5 μM Stx1A H3 domain. (D) Fold of activation of the initial rate of liposome fusion reaction in a dose–response experiment. Munc18-wt (5 μM) and different concentrations of Stx1A H3 domain were coincubated with t-/v-liposomes on ice for 3 h, which was followed by the fusion assay. (E) Order of addition experiment in which standard and preassembled liposome fusion experiments were performed as described in Figure 3; in this case, Stx1A-H3 was added either during the preincubation step or after the preincubation.

Munc18-1 activation by preventing Munc18-1 from binding to the preassembled SNARE complex during the preincubation step.

In t-liposomes, the majority of the Stx1A H3 domain is engaged in a heterodimer complex with SNAP-25. However, the Stx1A Habc domain might be free to interact with other partners. One possibility would be that the soluble Stx1A H3 domains we added into the system might form a "new Stx1A four-helix bundle" with the free Habc domain of the membrane embedded Stx1A. This "new Stx1A-four-helix bundle" may compete with the four-helix bundle SNARE complex for binding Munc18-1. To address this question, we tested the effect of adding soluble Stx1A H3 domain to the liposome fusion assay using liposomes containing a truncated version of t-SNARE without the Stx1A Habc domain (t-SNAREΔH_{abc}), but preserving the Stx1A N-peptide region (Shen *et al.*, 2007). We found that the Stx1A H3 domain still inhibited Munc18-1 activation of liposome fusion (Figure S4B). This establishes that the Stx1A H3 domain directly competes with the SNARE four-helix bundle for binding to Munc18-1.

The interaction of the C-terminal half of the Stx1A H3 domain with Munc18-1 central cavity is critical for competing with SNARE-complex binding and inhibiting Munc18 activation of fusion

In agreement with our biochemical data shown in Figure 4A, previous studies have shown that mutations in the Stx1A H3 domain impair Munc18 binding (Wu *et al.*, 1999). To characterize in detail the Stx1A H3 domain–Munc18 interaction, we studied the effect on Munc18-4M activation of the liposome fusion assay when the Stx1A H3 domain is added. Our findings showed that liposome fusion activation of Munc18-4M was largely insensitive to the addition of the Stx1A H3 domain (Figure 5, A and B). Similar results were obtained when we tested the activation of Munc18-4M on preassembled SNARE complexes (Figure S4C). To further prove this hypothesis, we mutated the complementary residues on the Stx1A H3 domain (D231A/E234A/N236A/D242A, Stx1A H3-4M) that interact with the residues mutated in Munc18-4M. Addition of soluble Stx1A H3-4M domain to the liposome fusion reaction in the presence of Munc18-wt did not affect the Munc18-1 activation of the fusion reaction in either standard or preassembled fusion conditions (Figures 5, C and D, and S4D). Altogether, these results strongly indicate that the Stx1A H3 domain can compete with the four-helix bundle SNARE complex for binding to the central cavity of Munc18-1, thus inhibiting the activation role of Munc18-1 in the SNARE-mediated membrane fusion.

DISCUSSION

In the present work, we provide direct evidence that the essential roles of Munc18-1 in trafficking Stx1A to the plasma membrane, as well as during the late steps of neurotransmitter release, rely on the interaction of the central cavity of Munc18-1 with either Stx1A or the SNARE complex. We show that some residues participating in each

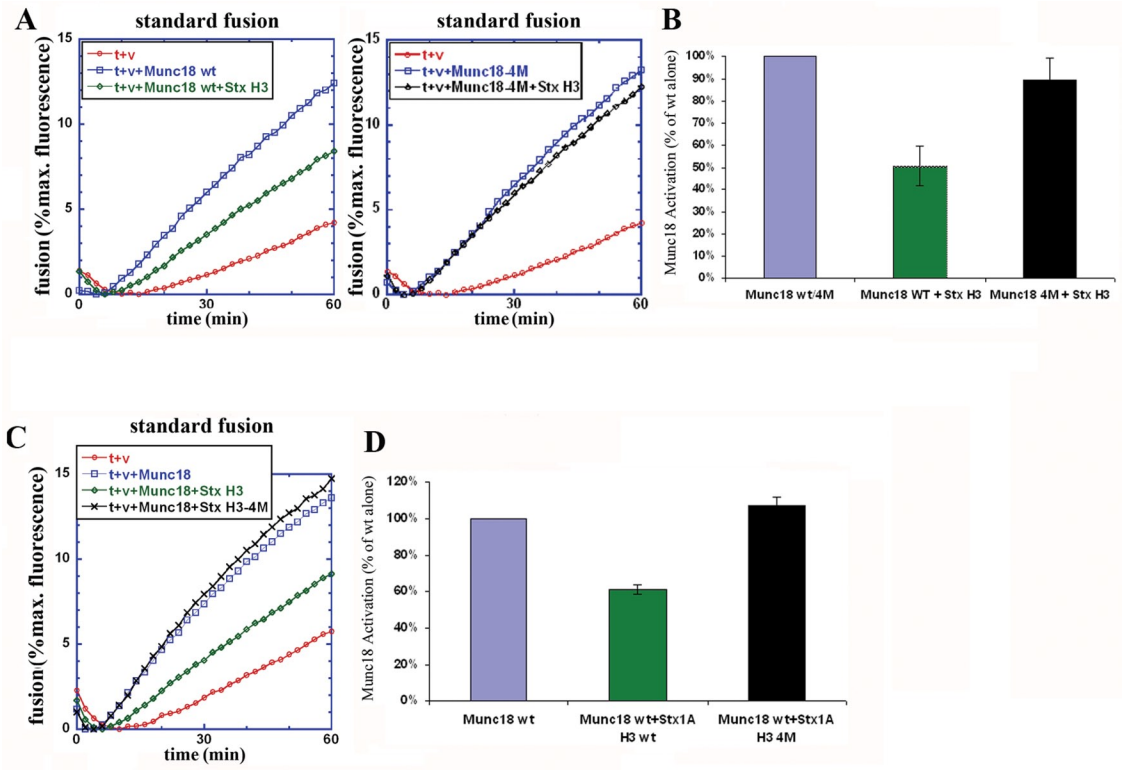

FIGURE 5: Stx1A H3 domain inhibition of Munc18 activation depends on the binding of its C-terminal region to the Munc18 central cavity. (A) Standard liposome fusion reactions performed in the absence or presence of 5 μM Stx1A H3 domain and Munc18-wt or Munc18-4M. Both panels show the same data for the "v+t" condition, since they were run in a single experiment for multiple times. (B) Inhibition effect of Stx1A H3 domain to Munc18-wt or Munc18-4M mutant on activation of liposome fusion. The maximum initial speed (within first 20 min) of liposome fusion in the presence of 5 μM Munc18 (wt or 4M) was calculated and set as 100%; the maximum initial speed in the presence of Stx1A H3 was measured and converted to the percentage of Munc18 activation. (C) Standard liposome fusion was carried out in the absence or presence of 5 μM Munc18-wt and 5 μM of Stx H3-wt or Stx1A H3-4M mutant (D231A/E234A/N236A/D242A). (D) Inhibition of Stx1A H3-wt, but not of Stx1A 4M, onto Munc18-wt activation of liposome fusion.

interaction are not shared between these two binding modes. Mutation of residues R39/K46/M47/K63 located within Munc18-1's central cavity remarkably reduced Munc18/Stx1A interaction, but had no effect on the Munc18–SNARE complex interaction. Rescue experiments using Munc18-1/-2 double-knockdown cells, showed that Munc18-4M cannot restore the normal trafficking of Stx1A to the plasma membrane but can support hGH secretion when Stx1A is overexpressed.

Munc18 has been intensively studied, and many interesting phenotypes have been identified for different mutants; however, most of these mutants have lost the interaction with either Stx1A or SNARE complex, as well as the ability to regulate SNARE-complex assembly. The Munc18-4M mutant we described here is a novel mutant distinct from any other Munc18 mutants previously described. For instance, the well-characterized Munc18 E59K (Deak *et al.*, 2009), which abrogate the interaction with residues in the Stx1A-Habc domain, displays a reduced binding for Stx1A, lacks the activation function in liposome fusion assay, and fails to regulate vesicle release in vivo (Shen *et al.*, 2007; Deak *et al.*, 2009; Han *et al.*, 2009). Munc18 F115E/E132A is another valuable mutant that abrogates the interaction with Stx1A N-peptide. This mutant shows a modest reduction in binding to Stx1A alone, but has a dramatically reduced binding to the SNARE complex (Malintan *et al.*, 2009). Elimination of the interaction Munc18 F115/E132-Stx1A N-peptide also severely affects Munc18 activation of fusion in vitro (Shen *et al.*, 2007). Therefore the Munc18-4M mutant described in this work has unique properties in dissecting the Munc18 chaperone function from the fusion regulation function.

Previous studies reported that Munc18-1 can bind both monomeric Stx1A and the SNARE complex (Misura *et al.*, 2000; Dulubova *et al.*, 2007; Shen *et al.*, 2007, 2010; Deak *et al.*, 2009). The calculated binding affinity of Munc18-1 and Stx1A (nM range) is much higher than that of Munc18-1 and SNARE complex (μM range; Hata *et al.*, 1993; Burkhardt *et al.*, 2008; Xu *et al.*, 2010). The tight interaction of Munc18-1 and the closed form of Stx1A could prevent Stx1A from forming wrong complexes with noncognate SNARE proteins during its trafficking, ensuring that Stx1A exerts its function at the presynaptic membrane (Medine *et al.*, 2007). Our results are consistent with those of others, which showed that the deletion or mutation of the Stx1A H3 domain dramatically decreased the binding affinity of Stx1A to Munc18-1 (Wu *et al.*, 1999; Burkhardt *et al.*, 2008). However, it was unclear from these previous studies whether the change in the binding affinity is due to the disruption of the Stx1A four-helix bundle structure or to the deletion of the Stx1A H3 domain. In this study, we introduced point mutations rather than domain deletion to keep the overall structure of Stx1A, and our data clearly established the importance of the Stx1A H3 domain (C-terminal half) in Munc18-Stx1A interactions.

Previous biochemical, functional, and structural studies have shown that Munc18-1 can also bind the SNARE complex, specifically through a direct interaction with the C-terminal region of VAMP2 and the Stx1A N-peptide (Dulubova *et al.*, 2007; Shen *et al.*, 2007, 2010; Xu *et al.*, 2010), but the intermolecular interactions within this complex remained unclear. Our studies showed that Munc18-4M displayed a reduced interaction with monomeric Stx1A, but it was still able to bind the SNARE complex in the liposome flotation assay and to activate liposome fusion as strongly as Munc18-wt. These data suggest that Munc18-1 binds to Stx1A or to the SNARE complex differently via its central cavity.

In the Munc18-Stx1A heterodimer, the C-terminal half of the Stx1A H3 domain is twisted and inserted deeply into the central cavity of Munc18-1. The close contacts between them greatly contribute to the tight interaction. However, this conformation of Stx1A H3 is not compatible with the four-helix bundle of the SNARE complex. Therefore the C-terminal half of the Stx1A H3 domain should dissociate from the Munc18-1 central cavity either before or during the assembly of the Stx1A H3 domain with SNAP25 and VAMP2 into a four-helix bundle. This idea is supported by both NMR studies in which the MUN domain of Munc13-1 facilitates the transition between the two binding modes of Munc18 (Ma *et al.*, 2011) and by studies on the intact plasma membrane sheets that have shown that SNAP25 and VAMP2 can displace Munc18-1 from the heterodimer Munc18-Stx1A to form SNARE complexes (Zilly *et al.*, 2006).

In a recent study, it has been proposed that the Stx1A N-peptide and the SNARE four-helix bundle constitute the minimal components for Munc18-1 activation of fusion, while the Habc domain of Stx1A is dispensable (Shen *et al.*, 2010). Combining previous models with our results, we propose a transition model between the two distinct binding modes: because the Stx1A Habc domain is flexible and dynamic, it could either bind the Stx1A H3 domain to form a "closed" conformation (Figure 6A), or it could move out of the cavity to adopt a transient "open" conformation while the Stx1A H3 domain is always bound to Munc18-1 (Figure 6B). Since Munc18-1–Stx1A H3 domain is a weak affinity interaction, the intermediate (Figure 6B) in this model is most likely to be transient. This would permit, in the presence of SNAP-25 and VAMP2, SNARE complexes to start zippering from the N-terminal region of the Stx1A H3 domain, which is freely accessible for SNARE proteins, while the C-terminal half of the Stx1A H3 domain dissociates from Munc18-1 before or during the formation of the SNARE four-helix bundle (Figure 6C). During this transition, key residues within Munc18 central cavity, such as E59, could switch from interacting with Stx1-Hc domain to starting to make contact with the SNARE complex, using epitopes other than the Stx1-Habc domain. Thus the Stx1A N-peptide might be responsible for linking these two distinct modes by holding Stx1A in place during SNARE-complex assembly. At this stage, the transition would be largely favorable to SNARE-complex assembly, due to strong cooperative interactions of Munc18-1 with the C-terminal region of VAMP2 (Shen *et al.*, 2007; Xu *et al.*, 2010), SNAP25 (Rodkey *et al.*, 2008) and both vesicular and target membranes (Xu *et al.*, 2010). Thus this model would assure an N- to C-terminal polarized assembly of SNARE complexes, and it would also explain why there is no formation of anti-parallel SNARE complexes in vivo, which has sometimes been observed in experiments in vitro (Melia *et al.*, 2002; Weninger *et al.*, 2003).

Other factors, such as Munc13 and arachidonic acid, have been implicated during the transition from the closed to open conformation of Stx1A (Rickman and Davletov, 2005; Xu *et al.*, 2010; Ma *et al.*, 2011). However, it is not clear whether these factors are essential or whether they only assist Munc18-1 during the transition. Further studies may be able to shed more light on this mechanism.

In conclusion, our findings suggest that Munc18-1 executes its dual roles by using two different binding modes to interact with Stx1A and SNARE complexes via its central cavity. Thus Munc18-1 is crucial during the membrane fusion reaction and also plays an essential role in calcium-regulated membrane fusion. The data presented here provide substantial insights into understanding the complex mechanism by which Munc18-1 actively cooperates with SNARE proteins to induce membrane fusion, and led us to propose a model for the transition between the two distinct binding modes in which the Stx1A H3 domain remains within the central cavity of Munc18 while it starts zippering with the other SNAREs, and Munc18 can therefore control and assist in SNARE-complex assembly during neurotransmitter release.

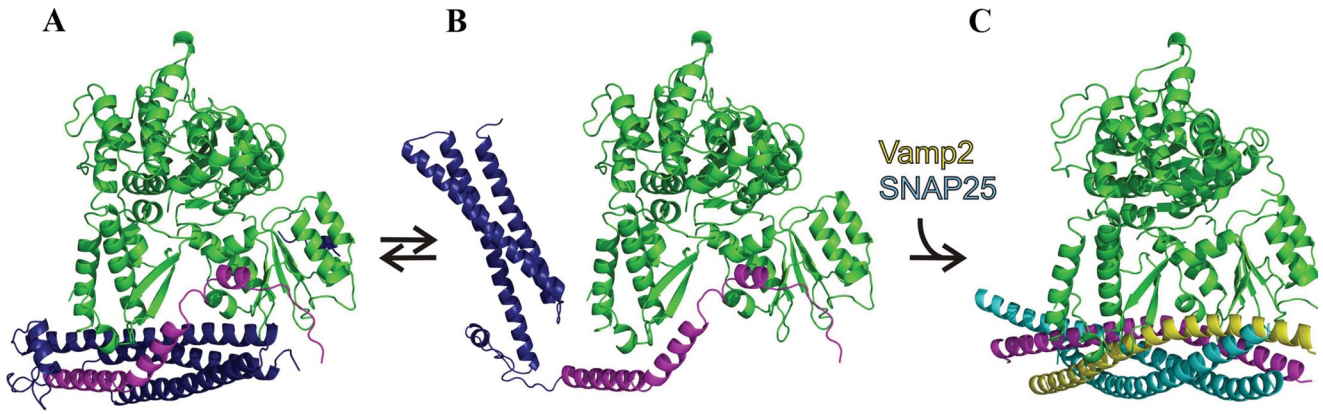

FIGURE 6: Proposed model of the transition between the distinct binding modes of Munc18/Stx1A and Munc18/SNARE complexes. (A) Munc18 (green) binds the closed form of Stx1A through the Habc domain (blue), the H3 domain (purple), and the N-peptide (blue). The four-helix bundle and the C-terminal half of Stx1A H3 domain are crucial for this high-affinity binding mode. (B) Munc18 binds the "open" form of Stx1A: the Habc domain is flexible and dynamic, and it may transiently move out of the Munc18 central cavity, whereas the H3 domain still binds to the central cavity. "Open" Stx1A is ready to assemble into the SNARE complex with SNAP-25 and VAMP2 by the "N- to C-terminal" direction. N-peptide (not shown) still binds Munc18 and may play an important role at this stage by presumably stabilizing Stx1A bound to Munc18. (C) Munc18 binds SNARE complex, involving both the Munc18 central cavity/SNARE four-helix bundle interaction and Munc18/Stx1A-N-peptide (Stx1A Habc domain and N-peptide are not shown).

MATERIALS AND METHODS

Protein expression and purification

Full-length t-SNARE Stx1A/SNAP 25 (pTW34) and truncated t-SNARE (pTW34ΔH_{abc}, kindly provided by Jingshi Shen, University of Colorado, Boulder, CO) were expressed and purified as previously described (Melia *et al.*, 2002; Shen *et al.*, 2010). Full-length mouse Vamp2 cloned into pet28-small ubiquitin-like modifier (pet28-SUMO) vector (kindly provided by Jingshi Shen), Munc18-wt, and Munc18-4M were expressed and purified as previously described (Shen *et al.*, 2007). In brief, all His-tagged proteins were expressed and purified according to Qiagen's *The QIAexpressionist* handbook (Valencia, CA). For SUMO-His-tagged protein, on-column cleavage is performed with SUMO protease overnight at 4°C. Constructs containing point mutations were generated by using QuickChange site-directed mutagenesis kit (Stratagene, Agilent, Santa Clara, CA).

Proteoliposome reconstitution

All lipids were purchased from Avanti Polar Lipids (Alabaster, AL). SNARE proteins were reconstituted into proteoliposomes by detergent dilution and isolated on a Nycodenz density gradient flotation, as previously described (Weber *et al.*, 1998). For t-SNARE proteoliposome preparation, a 1:500 protein:lipid ratio was used with the lipid mixture POPC (1-palmitoyl, 2-oleoyl phosphatidylcholine)/DOPS (1,2-dioleoyl phosphatidylserine) (85:15). v-SNARE proteoliposomes were prepared at a 1:200 protein:lipid ratio with the lipid mixture POPC:DOPS:rhodamine-DPPE (*N*-(lissamine rhodamine B sulfonyl) 1,2-dipalmitoyl phosphatidylethanolamine):NBD-DPPE (*N*-(7-nitro-2,1,3-benzoxadiazole-4-yl)-1,2-dipalmitoyl phosphatidylethanolamine) (82:15:1.5:1.5).

Competition assay

The rat Stx1A H3 soluble domain (aa 191–253) was expressed as a GST fusion protein and purified using standard methods. Full-length Munc18-1-wt or Munc18-4M were expressed and purified, and the tag was cleaved as previously described (Shen *et al.*, 2007). SNARE complex was assembled using 6xHis-MBP-VAMP2 (aa 26–96), 6xHis-MBP-SNAP25N (aa 11–82), GST-SNAP25C (aa 141–203), and GST-Stx1A (aa 191–253). Tags were cleaved using either thrombin or tobacco etch virus protease for 6xHis-MBP or GST, respectively. To assemble the SNARE complex, all four proteins were mixed in equal molar ratios and incubated overnight at 4°C, as described in Kümmel *et al.* (2011). Binding reactions were performed in 500 µl of buffer containing 25 mM HEPES (pH 7.4), 100 mM NaCl, 0.1% NP40 (Sigma-Aldrich, St. Louis, MO), and 1 mM dithiothreitol at room temperature using 20 µg of soluble GST-Stx1A H3 domain, 75 nM Munc18-1 wt or Munc18-4M, and 25 µl of a 50:50 slurry of glutathione beads. After 2 h, SNARE complex was added either at 37.5, 75, 150, or 300 nM to compete with the Stx1A H3 domain for binding to Munc18-1. The pulldown was allowed to proceed for another 2 h. Beads were washed five times and boiled in sample buffer, and proteins were loaded onto an SDS–PAGE for Western blot analysis using an anti–Munc18-1 antibody (Sigma).

Liposome flotation assay

Liposome flotation assay was carried out as previously described (Shen *et al.*, 2007). Briefly, t-liposomes were incubated with cdv2 at 4°C overnight, then Munc18 was added into the mixture, which was incubated for another 1 h at 4°C. The liposome–protein mixture (equal volume of 80% Nycodenz [wt/vol] in reconstitution buffer) was transferred to five 41-mm centrifuge tubes. The liposomes were overlaid first with 200 µl each of 35 and 30% Nycodenz and then with 20 µl reconstitution buffer. Centrifugation was performed at 48,000 rpm for 4 h. Samples were collected from the 0/30% Nycodenz interface (two 20-µl samples) and analyzed by SDS–PAGE.

Pulldown assay

His-tagged t-SNARE was coexpressed and bound to Ni-nitrilotriacetic acid (Ni-NTA) beads and then used to pull down 20 µg Munc18-wt or Munc18-4M mutant proteins. After three washes with buffer containing 20 mM imidazole, the protein samples were analyzed by SDS–PAGE and Coomassie staining. To form the SNARE complex, His-tagged t-SNARE and an extra amount of cdv2 were incubated at 4°C overnight. The next day, the SNARE complexes were purified with Ni-NTA beads and a pulldown assay was performed as described above.

Liposome fusion assay

A mixture of 45-µl unlabeled t-SNARE liposomes and 5-µl labeled v-SNARE liposomes was used for the fusion assay, as previously described (Weber *et al.*, 1998). Fusion was measured in a 96-well FluoroNunc PolySorp plate (Thermo Scientific, Lafayette, CO) at 37°C as the increase in 7-nitro-2-1,3-benzoxadiazol-4-yl (NBD)-fluorescence at 538 nm every 2 min. At 120 min of the reaction, 10 µl 2.5% *N*-dodecylmaltoside was added to the liposomes and data continued to be collected for another 40 min to get the maximum NBD signal. Raw NBD-fluorescence data were converted into the percentage of maximum NBD signal. Standard liposome fusion or preassembled liposome fusion with Munc18 was done as previously described (Shen *et al.*, 2007, 2010). The maximum fusion rate within the first 20 min of the reaction from three independent experiments was used to calculate the initial rate of a fusion reaction. For competition experiments (Figures 4, C–E, and 5), different concentrations of Stx1A H3 domain (as indicated) were used during the coincubation with Munc18 and t-/v-liposomes for 3 h on ice, followed by the fusion reaction. A high concentration of Stx1A H3 domain could not be achieved, most likely because of formation of oligomers in solution (Misura *et al.*, 2001), which may limit Stx1A H3 domain inhibition of Munc18 activation of liposome fusion.

coIP

Rat Stx1A, rat Munc18-wt, and Munc18 mutants were subcloned into pcDNA6/V5-HisA vector. Stx1A wt or mutants were cotransfected with either Munc18-wt or Munc18-4M into HeLa cells. Twenty-four hours after transfection, cells were lysed using lysis buffer (20 mM HEPES, 100 mM NaCl, pH 8.0) containing 1% Triton X-100, which was followed by centrifugation at 12,000 rpm for 15 min. Supernatants were collected and incubated with HPC-1 anti-Stx1A monoclonal antibody for 2 h at 4°C. Protein A-agarose beads were added to the supernatants and incubated for another 2 h. Complexes bound to the beads were pelleted by centrifugation followed by three washes with lysis buffer containing 0.5% Triton X-100. The precipitates were tested by Western blotting using rabbit anti Munc18 antibody (Sigma).

ITC

ITC was performed on a VP-ITC 200 (MicroCal, Piscataway, NJ) at 25°C. Samples were dialyzed against buffer (100 mM NaCl, 20 mM HEPES, 0.5 mM Tris(2-carboxyethyl)phosphine, pH 7.4). The data were integrated and analyzed with MicroCal Origin 9.0 using a single-site binding model, yielding the equilibrium association constant K_a, the enthalpy of binding DH, and the stoichiometry N.

Munc18 knockdown PC12 cells maintenance and immunostaining

PC12 Munc18-1/-2 double-knockdown stable cell line (DKD16) and the control cell line (C8) were kindly provided by Shuzo Sugita (University Health Network, Toronto, Ontario, Canada). These cells were maintained as previously described (Han *et al.*, 2009). The day before transfection, PC12 cells were seeded in 24-well plates containing poly-lysine coated glass coverslips. Cells were transfected with the indicated constructs using Lipofectamine 2000 (Invitrogen, Carlsbad, CA). Twenty-four hours after transfection, differentiation was induced with 50 ng/ml nerve growth factor for 2 d. Cells were washed with phosphate-buffered saline (PBS) buffer and fixed for 10 min with PBS buffer containing 4% paraformaldehyde. Cells were permeabilized with PBS buffer containing 0.3% Triton X-100, and then cells were blocked with 3% bovine serum albumin (BSA) in PBS buffer for 30 min at room temperature. Immunostaining of cells was performed by using HPC-1 antibody against Stx1 (1:2000 dilution), which was followed by three washes with PBS buffer. Alexa Fluor 488 goat anti-mouse antibody was used as a secondary antibody at 1:500 dilution. Coverslips were washed three times with PBS and mounted with Prolong Gold antifade reagent (Invitrogen). Images were collected with a Zeiss LSM 510 confocal microscope (Zeiss).

hGH secretion assay

C8 or DKD16 PC12 cells were plated in six-well plates; 3–4 d after plating, the cells were cotransfected with a plasmid coding for hGH-yellow fluorescent protein (YFP) and either Munc18-wt, Munc18-4M, Munc18-4M, and Stx1A or mock-transfected. Cells were incubated for 3–4 d and then transferred into 24-well plates for the secretion experiment. The cells were washed once with physiological saline solution (PSS) containing 145 nM NaCl, 2.2 mM KCl, 2.2 mM $CaCl_2$, 0.5 mM $MgCl_2$, 5.6 mM glucose, and 15 mM HEPES, pH 7.4. hGH secretion was stimulated with 200 µl of PSS or high K^+-PSS containing 81 mM NaCl and 70 mM KCl. Secretion was terminated after a 15-min incubation at 37°C by chilling to 0°C, and samples were centrifuged at 4°C for 3 min at 5000 rpm. Medium was collected for hGH ELISA and measured according to the vendor's protocol (Roche Diagnostics, Indianapolis, IN).

ACKNOWLEDGMENTS

We thank Jingshi Shen (University of Colorado) for providing SUMO-Munc18-1-pet28 clone and some other clones; Shuzo Sugita (University Health Network) for providing PC12 Munc18-1/-2 double-knockdown stable cell line and control cell line; Yingke Xu for assistance in confocal microscopy; Yiying Cai for assistance in using CNS programs to calculate the distances among residues on Munc18 and stx1A; Stephanie Baguley for culturing and transfecting PC12 cells; James E. Rothman, Jingshi Shen, Shyam Krishnakumar, and Daniel Radoff for helpful discussions; and Lena Schroeder for reviewing the manuscript. We also thank the members of the Rothman laboratory.

REFERENCES

Arunachalam L *et al.* (2008). Munc18-1 is critical for plasma membrane localization of syntaxin1 but not of SNAP-25 in PC12 cells. Mol Biol Cell 19, 722–734.

Augustin I, Rosenmund C, Sudhof TC, Brose N (1999). Munc13-1 is essential for fusion competence of glutamatergic synaptic vesicles. Nature 400, 457–461.

Bonifacino JS, Lippincott-Schwartz J (2003). Coat proteins: shaping membrane transport. Nat Rev Mol Cell Biol 4, 409–414.

Brose N, Petrenko AG, Sudhof TC, Jahn R (1992). Synaptotagmin: a calcium sensor on the synaptic vesicle surface. Science 256, 1021–1025.

Brunger AT *et al.* (1998). Crystallography & NMR system: a new software suite for macromolecular structure determination. Acta Crystallogr D Biol Crystallogr 54, 905–921.

Burkhardt P, Hattendorf DA, Weis WI, Fasshauer D (2008). Munc18a controls SNARE assembly through its interaction with the syntaxin N-peptide. EMBO J 27, 923–933.

Carr CM, Rizo J (2010). At the junction of SNARE and SM protein function. Curr Opin Cell Biol.

Chung SH, Joberty G, Gelino EA, Macara IG, Holz RW (1999). Comparison of the effects on secretion in chromaffin and PC12 cells of Rab3 family members and mutantsEvidence that inhibitory effects are independent of direct interaction with Rabphilin3. J Biol Chem 274, 18113–18120.

Deak F, Xu Y, Chang WP, Dulubova I, Khvotchev M, Liu X, Sudhof TC, Rizo J (2009). Munc18-1 binding to the neuronal SNARE complex controls synaptic vesicle priming. J Cell Biol 184, 751–764.

Diao J, Su Z, Lu X, Yoon TY, Shin YK, Ha T (2010). Single-vesicle fusion assay reveals Munc18-1 binding to the SNARE core is sufficient for stimulating membrane fusion. ACS Chem Neurosci 1, 168–174.

Dulubova I, Khvotchev M, Liu S, Huryeva I, Sudhof TC, Rizo J (2007). Munc18-1 binds directly to the neuronal SNARE complex. Proc Natl Acad Sci USA 104, 2697–2702.
Dulubova I, Sugita S, Hill S, Hosaka M, Fernandez I, Sudhof TC, Rizo J (1999). A conformational switch in syntaxin during exocytosis: role of munc18. EMBO J 18, 4372–4382.
Fisher RJ, Pevsner J, Burgoyne RD (2001). Control of fusion pore dynamics during exocytosis by Munc18. Science 291, 875–878.
Gerber SH *et al*. (2008). Conformational switch of syntaxin-1 controls synaptic vesicle fusion. Science 321, 1507–1510.
Giraudo CG, Eng WS, Melia TJ, Rothman JE (2006). A clamping mechanism involved in SNARE-dependent exocytosis. Science 313, 676–680.
Giraudo CG, Garcia-Diaz A, Eng WS, Chen Y, Hendrickson WA, Melia TJ, Rothman JE (2009). Alternative zippering as an on-off switch for SNARE-mediated fusion. Science 323, 512–516.
Han L *et al*. (2009). Rescue of Munc18-1 and -2 double knockdown reveals the essential functions of interaction between Munc18 and closed syntaxin in PC12 cells. Mol Biol Cell 20, 4962–4975.
Hata Y, Slaughter CA, Sudhof TC (1993). Synaptic vesicle fusion complex contains *unc-18* homologue bound to syntaxin. Nature 366, 347–351.
Hu C, Ahmed M, Melia TJ, Sollner TH, Mayer T, Rothman JE (2003). Fusion of cells by flipped SNAREs. Science 300, 1745–1749.
Khvotchev M, Dulubova I, Sun J, Dai H, Rizo J, Sudhof TC (2007). Dual modes of Munc18-1/SNARE interactions are coupled by functionally critical binding to syntaxin-1 N terminus. J Neurosci 27, 12147–12155.
Kümmel D, Krishnakumar S, Radoff D, Li F, Giraudo CG, Pincet F, Rothman JE, Reinisch K (2011). Complexin cross-link pre-fusion SNAREs into a zig-zag array: a structure-based model for complexin clamping. Nat Struct Mol Biol 18, 927–933.
Ma C, Li W, Xu Y, Rizo J (2011). Munc13 mediates the transition from the closed syntaxin-Munc18 complex to the SNARE complex. Nature Struct Mol Biol.
Malintan NT, Nguyen TH, Han L, Latham CF, Osborne SL, Wen PJ, Lim SJ, Sugita S, Collins BM, Meunier FA (2009). Abrogating Munc18-1-SNARE complex interaction has limited impact on exocytosis in PC12 cells. J Biol Chem 284, 21637–21646.
Medine CN, Rickman C, Chamberlain LH, Duncan RR (2007). Munc18-1 prevents the formation of ectopic SNARE complexes in living cells. J Cell Sci 120, 4407–4415.
Melia TJ, Weber T, McNew JA, Fisher LE, Johnston RJ, Parlati F, Mahal LK, Sollner TH, Rothman JE (2002). Regulation of membrane fusion by the membrane-proximal coil of the t-SNARE during zippering of SNAREpins. J Cell Biol 158, 929–940.
Misura KM, Scheller RH, Weis WI (2000). Three-dimensional structure of the neuronal-Sec1-syntaxin 1a complex. Nature 404, 355–362.
Misura KM, Scheller RH, Weis WI (2001). Self-association of the H3 region of syntaxin 1A. Implications for intermediates in SNARE complex assembly. J Biol Chem 276, 13273–13282.
Rathore SS, Bend EG, Yu H, Hammarlund M, Jorgensen EM, Shen J (2010). Syntaxin N-terminal peptide motif is an initiation factor for the assembly of the SNARE-Sec1/Munc18 membrane fusion complex. Proc Natl Acad Sci USA 107, 22399–22406.
Reim K, Mansour M, Varoqueaux F, McMahon HT, Sudhof TC, Brose N, Rosenmund C (2001). Complexins regulate a late step in Ca^{2+}-dependent neurotransmitter release. Cell 104, 71–81.
Rickman C, Davletov B (2005). Arachidonic acid allows SNARE complex formation in the presence of Munc18. Chem Biol 12, 545–553.
Rickman C, Medine CN, Bergmann A, Duncan RR (2007). Functionally and spatially distinct modes of munc18-syntaxin 1 interaction. J Biol Chem 282, 12097–12103.
Rodkey TL, Liu S, Barry M, McNew JA (2008). Munc18a scaffolds SNARE assembly to promote membrane fusion. Mol Biol Cell 19, 5422–5434.
Rosenmund C, Rettig J, Brose N (2003). Molecular mechanisms of active zone function. Current Opin Neurobiol 13, 509–519.
Rowe J, Calegari F, Taverna E, Longhi R, Rosa P (2001). Syntaxin 1A is delivered to the apical and basolateral domains of epithelial cells: the role of munc-18 proteins. J Cell Sci 114, 3323–3332.
Rowe J, Corradi N, Malosio ML, Taverna E, Halban P, Meldolesi J, Rosa P (1999). Blockade of membrane transport and disassembly of the Golgi complex by expression of syntaxin 1A in neurosecretion-incompetent cells: prevention by rbSEC1. J Cell Sci 112,, 1865–1877.
Salaun C, James DJ, Greaves J, Chamberlain LH (2004). Plasma membrane targeting of exocytic SNARE proteins. Biochim Biophys Acta 1693, 81–89.
Scott BL, Van Komen JS, Irshad H, Liu S, Wilson KA, McNew JA (2004). Sec1p directly stimulates SNARE-mediated membrane fusion in vitro. J Cell Biol 167, 75–85.
Shen J, Rathore SS, Khandan L, Rothman JE (2010). SNARE bundle and syntaxin N-peptide constitute a minimal complement for Munc18-1 activation of membrane fusion. J Cell Biol 190, 55–63.
Shen J, Tareste DC, Paumet F, Rothman JE, Melia TJ (2007). Selective activation of cognate SNAREpins by Sec1/Munc18 proteins. Cell 128, 183–195.
Sorensen JB (2009). Conflicting views on the membrane fusion machinery and the fusion pore. Annu Rev Cell Dev Biol 25, 513–537.
Sudhof TC (2004). The synaptic vesicle cycle. Annu Rev Neurosci 27, 509–547.
Sudhof TC, Rothman JE (2009). Membrane fusion: grappling with SNARE and SM proteins. Science 323, 474–477.
Sutton RB, Fasshauer D, Jahn R, Brunger AT (1998). Crystal structure of a SNARE complex involved in synaptic exocytosis at 2.4 A resolution. Nature 395, 347–353.
Toonen RF, Verhage M (2007). Munc18-1 in secretion: lonely Munc joins SNARE team and takes control. Trends Neurosci 30, 564–572.
Tucker WC, Weber T, Chapman ER (2004). Reconstitution of Ca^{2+}-regulated membrane fusion by synaptotagmin and SNAREs. Science 304, 435–438.
Verhage M *et al*. (2000). Synaptic assembly of the brain in the absence of neurotransmitter secretion. Science 287, 864–869.
Weber T, Zemelman BV, McNew JA, Westermann B, Gmachl M, Parlati F, Sollner TH, Rothman JE (1998). SNAREpins: minimal machinery for membrane fusion. Cell 92, 759–772.
Weimer RM, Richmond JE, Davis WS, Hadwiger G, Nonet ML, Jorgensen EM (2003). Defects in synaptic vesicle docking in *unc-18* mutants. Nat Neurosci 6, 1023–1030.
Weninger K, Bowen ME, Chu S, Brunger AT (2003). Single-molecule studies of SNARE complex assembly reveal parallel and antiparallel configurations. Proc Natl Acad Sci USA 100, 14800–14805.
Wu MN, Fergestad T, Lloyd TE, He Y, Broadie K, Bellen HJ (1999). Syntaxin 1A interacts with multiple exocytic proteins to regulate neurotransmitter release in vivo. Neuron 23, 593–605.
Wu MN, Littleton JT, Bhat MA, Prokop A, Bellen HJ (1998). ROP, the *Drosophila* Sec1 homolog, interacts with syntaxin and regulates neurotransmitter release in a dosage-dependent manner. EMBO J 17, 127–139.
Xu Y, Su L, Rizo J (2010). Binding of Munc18-1 to synaptobrevin and to the SNARE four-helix bundle. Biochemistry 49, 1568–1576.
Zilly FE, Sorensen JB, Jahn R, Lang T (2006). Munc18-bound syntaxin readily forms SNARE complexes with synaptobrevin in native plasma membranes. PLoS Biol 4, e330.